ISSN 1674-1056
http://cpb.iphy.ac.cn
http://iopscience.iop.org/cpb
中国物理 B
Chinese Physics
中国物理 Chinese Physics B

# A new way to construct topological invariants of non-Hermitian systems with the non-Hermitian skin effect

J S Liu(刘建森), Y Z Han(韩炎桢), C S Liu(刘承师)

**Citation:**Chin. Phys. B . 2020, 29(1): 010302 . **doi:** 10.1088/1674-1056/ab5937
Journal homepage: http://cpb.iphy.ac.cn; http://iopscience.iop.org/cpb

**What follows is a list of articles you may be interested in**

---

## Topological phases of a non-Hermitian coupled SSH ladder

J S Liu(刘建森), Y Z Han(韩炎桢), C S Liu(刘承师)

Chin. Phys. B . 2019, 28(10): 100304 . **doi:** 10.1088/1674-1056/ab3f94

## Phase diagram of interacting fermionic two-leg ladder with pair hopping

Wan-Li Liu(刘万里), Tian-Zhong Yuan(原天忠), Zhi Lin(林志), Wei Yan(闫伟)

Chin. Phys. B . 2019, 28(2): 020303 . **doi:** 10.1088/1674-1056/28/2/020303

## Topologically protected edge gap solitons of interacting Bosons in one-dimensional superlattices

Xi-Hua Guo(郭西华), Tian-Fu Xu(徐天赋), Cheng-Shi Liu(刘承师)

Chin. Phys. B . 2018, 27(6): 060307 . **doi:** 10.1088/1674-1056/27/6/060307

## Rotational symmetry of classical orbits, arbitrary quantization of angular momentum and the role of the gauge field in two-dimensional space

Xin Jun-Li,Liang Jiu-Qing

Chin. Phys. B . 2012, 21(4): 040303 . **doi:** 10.1088/1674-1056/21/4/040303

## New theorem relating two-mode entangled tomography to two-mode Fresnel operator

Xie Chuan-Mei, Fan Hong-Yi

Chin. Phys. B . 2012, 21(1): 010302 . **doi:** 10.1088/1674-1056/21/1/010302

---

# A new way to construct topological invariants of non-Hermitian systems with the non-Hermitian skin effect*

J S Liu(刘建森), Y Z Han(韩炎桢), and C S Liu(刘承师)†

*Hebei Key Laboratory of Microstructural Material Physics, School of Science, Yanshan University, Qinhuangdao* 066004, *China*

(Received 16 October 2019; revised manuscript received 13 November 2019; accepted manuscript online 20 November 2019)

The non-Hermitian skin effect breaks the conventional bulk–boundary correspondence and leads to non-Bloch topological invariants. Inspired by the fact that the topological protected zero modes are immune to perturbations, we construct a partner of a non-Hermitian system by getting rid of the non-Hermitian skin effect. Through adjusting the imbalance hopping, we find that the existence of zero-energy boundary states still dictate the bulk topological invariants based on the band-theory framework. Two non-Hermitian Su–Schrieffer–Heeger (SSH) models are used to illuminate the ideas. Specially, we obtain the winding numbers in analytical form without the introduction of the generalized Brillouin zone. The work gives an alternative method to calculate the topological invariants of non-Hermitian systems.

**Keywords:** non-Hermitian skin effect, Su–Schrieffer–Heeger (SSH) model, bulk–boundary correspondence, topological invariant

**PACS:** 03.65.Vf, 05.70.Fh, 64.70.Tg **DOI:** 10.1088/1674-1056/ab5937

## 1. Introduction

The bulk–boundary correspondence is the central principle of topological matter where the existence of robust edge states is attributed to the nontrivial bulk topological invariants on the band-theory framework.[1,2] However, numerical results show that open-boundary spectra of some non-Hermitian systems look quite different from those of periodic-boundary.[3–6] It indicates that the bulk–boundary correspondence is true for Hermitian systems and is breakdown completely for some non-Hermitian systems. General topological invariants are needed to depict the non-Hermitian bulk–boundary correspondence. To systematically understand the physical properties of symmetry-protected topological phases, a lot of effort has been paid to systematic classifications of non-Hermitian systems.[7–9]

The issue is resolved by considering the non-Hermitian skin effect which causes all eigenstates to localize exponentially to boundaries, regardless of the topological edge states and bulk states.[10–14] A complex-valued wave vector is introduced to construct the generalized Brillouin zone to capture the unique feature of non-Hermitian bands. The real part of the wave vector is from the periodicity of the system according to the Bloch theorem. The non-Hermitian skin effect determines the imaginary part of the complex-valued wave vector. A generalized bulk–boundary correspondence is set up theoretically by the introduction of the non-Bloch winding number in the one-dimensional (1D) non-Hermitian Su–Schrieffer–Heeger (SSH) model[10–13] and the non-Bloch Chern numbers in the two-dimensional (2D) non-Hermitian Chern insulators.[11,14] Experimentally, the non-Hermitian bulk–boundary correspondence has been demonstrated in discrete-time non-unitary quantum-walk dynamics of single photons[15] and in topolectrical circuits.[16] However, except for a simple non-Hermitian SSH model where the non-Hermitian skin effect can be separated by a similarity transformation,[10] it is difficult to obtain the topological invariant in analytic form.

In fact, the non-Hermitian skin effect is due to the imbalance hopping in the left and right directions. The asymmetric couplings create effectively an imaginary gauge field. The nonzero imaginary magnetic flux breaks the conventional bulk–boundary correspondence and leads to a topological phase transition.[17] If the the non-Hermitian skin effect does not exist, such as the non-Hermitian system in the time-reversal symmetry-unbroken region[17–19] or with inversion symmetry,[20] it is unnecessary to separate the non-Hermitian skin effect, or to introduce the complex wave vector. The non-Hermitian topological invariants based on the Bloch theorem can accurately predict the topological phase transition. In particular, it is well known that the topological boundary states are protected by the symmetry of system and are immune to perturbations. It is reasonable to speculate that, for a class of non-Hermitian systems with non-Hermitian skin effect, there is a partner without non-Hermitian skin effect that shares the same topological phase diagrams. As such, the topological invariants of the original models with non-Hermitian skin effect can be obtained from their partners, which can be calculated in an easier way.

*Project supported by Hebei Provincial Natural Science Foundation of China (Grant Nos. A2012203174 and A2015203387) and the National Natural Science Foundation of China (Grant Nos. 10974169 and 11304270).

†Corresponding author. E-mail: csliu@ysu.edu.cn

© 2020 Chinese Physical Society and IOP Publishing Ltd 

In this paper, we use the 1D non-Hermitian SSH model and coupled non-Hermitian SSH model to verify the above ideas. Their partners are constructed by exchanging the strength of the hopping term of the adjacent unit cell in the right and left directions. Although the non-Hermitian skin effect disappears, the systems still have the non-Hermiticity. As shown in the numerical analysis, the topological structure of energy band of the deformed model Hamiltonian $H$ is the same as that of the prototype Hamilton where the non-Hermitian skin effect is present. We can obtain the topological phase transition points of the prototype Hamiltonian by studying its corresponding partner where the non-Hermitian skin effect is killed. In particular, the topological structure of energy band of the deformed model Hamiltonian $H$ is the same as that of the Hermitian operator $H^{\dagger}H$. It suggests that the topological invariants based on band-theory are effective to discuss the topological phase transitions. We give the topological phase transition point of the prototype Hamilton by solving its partner analytically.

## 2. Models

The partner of the 1D non-Hermitian SSH model is shown in Fig. 1(a). The non-Hermiticity is due to the introduction of $\gamma/2$ which changes the hopping term in the unit cell $i$ with different hopping strengths in the right direction $t_{i,\mathrm{R}} = t_i + (-1)^i \gamma/2$ and left direction $t_{i,\mathrm{L}} = t_i - (-1)^i \gamma/2$. The term $(-1)^i$ causes the imbalance hopping between the adjacent unit cells to be canceled and the non-Hermitian skin effect disappears in the model. The partner Hamiltonian actually fulfils the inverse or reflection symmetry. The non-Hermitian topological systems with reflection symmetry have no skin effect.[9] It should first emphasize that not all non-Hermiticity can be killed in this simple way. For example, non-Hermiticity is introduced in the $t_3$ hopping terms, i.e., $t_3 + \gamma/2$ (right to left) and $t_3 + \gamma/2$ (left to right).

The Bloch Hamiltonian reads $H = \psi_k^{\dagger} H_k \psi_k$ with

$$H_k = \begin{pmatrix} 0 & t_1 + \frac{\gamma}{2} & 0 & t_2 \mathrm{e}^{-\mathrm{i}k} + t_3 \\ t_1 - \frac{\gamma}{2} & 0 & t_2 & 0 \\ 0 & t_2 & 0 & \frac{t_1}{2} - \frac{\gamma}{2} \\ t_2 \mathrm{e}^{\mathrm{i}k} + t_3 & 0 & \frac{t_1}{2} + \frac{\gamma}{2} & 0 \end{pmatrix}, \tag{1}$$

where $\psi_k^{\dagger} = \left( a_k^{\dagger},\ b_k^{\dagger},\ c_k^{\dagger},\ d_k^{\dagger} \right)$ is the creation operation of the lattice (ABCD) shown in Fig. 1(a). As the prototype Hamiltonian, the model also has a chiral symmetry $\Sigma_z^{-1} H_k \Sigma_z = -H_k$ with $\Sigma_z = \sigma_0 \otimes \sigma_z$, where $\sigma_0$ and $\sigma_z$ are the unity matrix and the Pauli matrix, respectively. The chiral symmetry ensures that the eigenvalues of Hamiltonian $H_k$ appear in $(E_j, -E_j)$ pairs with $j = 1, 2$.

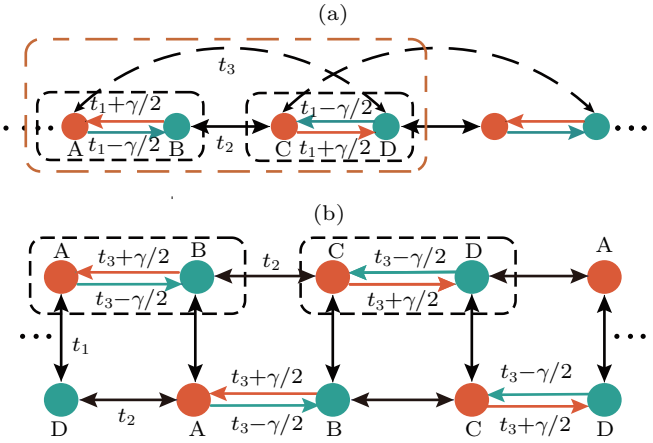



**Fig. 1.** (a) Non-Hermitian SSH model. The yellow-dashed box indicates the unit cell. (b) Coupled SSH model with alternating $t_1$, $t_2$ hoppings and a non-Hermitian $t_3 \pm \gamma/2$ hopping. The imbalance hopping between the adjacent unit cells (the black-dotted boxes) leads to the non-Hermitian skin effect disappearing.

Let us first discuss the simple case $t_3 = 0$, the four eigenvalues in analytic form are

$$\pm \left[ t_1^2 - \left(\frac{\gamma}{2}\right)^2 + t_2^2 \pm t_2 \sqrt{\frac{1}{\mathrm{e}^{\mathrm{i}k}} \left(\mathrm{e}^{\mathrm{i}k} + 1\right)^2 \left( t_1^2 - \left(\frac{\gamma}{2}\right)^2 \right)} \right]^{1/2}.$$

Since the energy gap must close at the phase transition points, we can determine the phase boundaries by the band-crossing condition $|E(k)| = 0$, which yields $t_1^2 = t_2^2 + (\gamma/2)^2$. The transition points are the same as those given in Ref. [10] where the non-Hermitian skin effect exists in the model.

To study the topological transitions, we diagonalize the Hamiltonian in Eq. (1) numerically under the open boundary condition. The open-boundary spectrum $|E|$ of the model is shown in Fig. 2(a) by blue lines. For comparison, we also present the open-boundary spectra of the prototype Hamiltonian with the non-Hermitian skin effect (red lines) given in Ref. [10]. Both of the open-boundary spectra have the same transition point of zero energy, which indicates further that the partner can be used to study the topological phase of the prototype model.

As shown in Refs. [21–23], if $H^{\dagger}H$ has a zero mode eigenstate, i.e., $H^{\dagger}H|\psi\rangle = 0|\psi\rangle = 0$, then $\langle\psi|H^{\dagger}H|\psi\rangle = 0$. We notice that $\left(\langle\psi|H^{\dagger}\right)^{\dagger} = H|\psi\rangle$, so $\langle\psi|H^{\dagger}H|\psi\rangle = |H|\psi\rangle|^2 = 0$ and $H|\psi\rangle = 0$. We also notice that the operator $H^{\dagger}H$ is a Hermitian operator and has the same periodicity with the Hamiltonian $H$. So the wave vector $k$ is a good quantum number and a real number.

To further understand the non-Hermitian skin effect, we present the open-boundary spectrum of $H^{\dagger}H$ in Fig. 2(b) by blue lines. The $H$ is the designed partner in Fig. 1(a) where no non-Hermitian skin effect is presented. The Hamilton $H$ (red lines) and the operator $H^{\dagger}H$ (blue lines) have the same topological transition points. However, in Fig. 2(c) for the case of the prototype Hamiltonian where the non-Hermitian skin effect is presented, the open-boundary spectrum of Hamiltonian

$H$ (red lines) is noticeably different from that of the operator $H^\dagger H$ (blue lines). It gives a direct evidence that the zero mode of $H^\dagger H$ is generally considered as the zero mode of $H$ of open boundary provided that the non-Hermitian skin effect is absent. The consistence of the open-boundary spectra of $H^\dagger H$ and $H$ in Fig. 2(b) indicates that the Bloch theorem is effective to discuss the non-Hermitian Hamiltonian in Eq. (1). It can also be taken as a useful benchmark to judge the previous non-Hermitian topological invariants in terms of the Bloch Hamiltonian.[3,21–28]

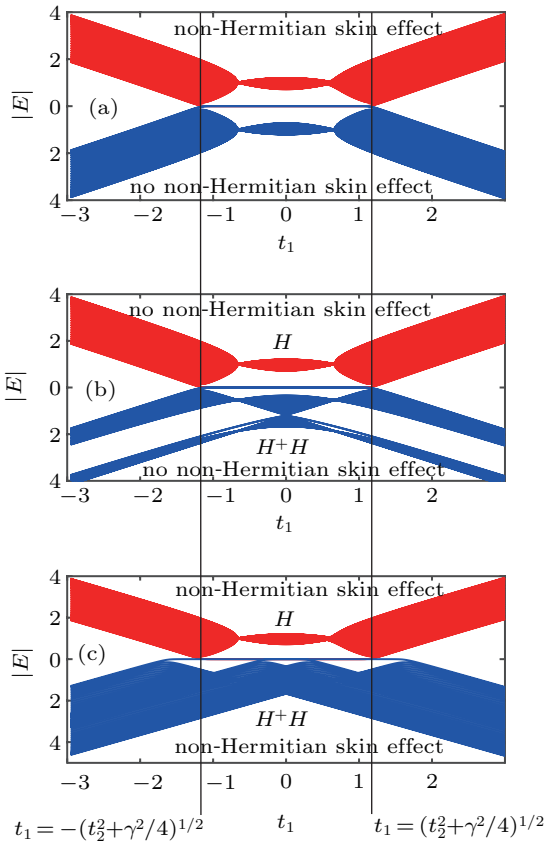



**Fig. 2.** Energy spectra of an open chain with length $L = 60$ as a function of $t_1$ by numerical diagonalization of the non-Hermitian SSH Hamiltonian: (a) red lines for the model in which the non-Hermitian skin effect exists as discussed in Ref. [10] and blue lines for its partner in which the non-Hermitian skin effect disappears as shown in Fig. 1(a). (b) Red lines for the partner Hamilton and blue lines for the corresponding Hermitian operator $H^\dagger H$. (c) Red lines for the prototype Hamilton and blue lines for the corresponding Hermitian operator $H^\dagger H$. The parameters are taken to be $t_2 = 1$, $t_3 = 0$, and $\gamma = 4/3$.

## 3. Topological invariant

It is well known that the winding number defined in terms of wavefunction determines the number of pairs of zero-energy edge states and can be used to distinguish different topological phases. When the non-Hermitan skin effect is present, the winding number must be defined in terms of wavefunction in the generalized Brillouin zone. Here the non-Hermitan skin effect is absent, the generalized Brillouin zone reduces to the conventional Brillouin zone, which is just the usual $k$ space. However, it is difficult to obtain the eigenfunction of Eq. (1) in analytic form. The definition of the winding number can also be relevant in the case of block off-diagonal Hamiltonian.[29,30] This winding number is used to predict the number of topological modes.

With the unitary transformation, the Hamiltonian $h_k$ in Eq. (1) can be brought into block off-diagonal form

$$\begin{aligned}\bar{H}_k &= UH_kU^{-1}\\ &= \begin{pmatrix} 0 & 0 & \frac{1}{2}\gamma+t_1 & t_3+t_2\mathrm{e}^{\mathrm{i}k} \\ 0 & 0 & t_2+t_3\mathrm{e}^{-\mathrm{i}k} & t_1-\frac{1}{2}\gamma \\ t_1-\frac{1}{2}\gamma & t_2+t_3\mathrm{e}^{\mathrm{i}k} & 0 & 0 \\ t_3+t_2\mathrm{e}^{-\mathrm{i}k} & \frac{1}{2}\gamma+t_1 & 0 & 0 \end{pmatrix}, \end{aligned} \tag{2}$$

where the unitary matrix

$$U = \begin{pmatrix} 0 & 0 & 0 & 1 \\ 0 & 1 & 0 & 0 \\ 0 & 0 & 1 & 0 \\ 1 & 0 & 0 & 0 \end{pmatrix}.$$

With the block off-diagonal Hamiltonian in Eq. (2), the winding number is defined by [29,30]

$$\begin{aligned}\mathcal{W} &= -\oint \frac{\mathrm{d}k}{2\pi\mathrm{i}}\partial_k \left\{ \ln\left[ \mathrm{Det}\begin{pmatrix} \frac{1}{2}\gamma+t_1 & t_3+t_2\mathrm{e}^{\mathrm{i}k} \\ t_2+t_3\mathrm{e}^{-\mathrm{i}k} & t_1-\frac{1}{2}\gamma \end{pmatrix}\right]\right\} \\ &= -\oint \frac{\mathrm{d}k}{2\pi\mathrm{i}}\partial_k \left\{ \ln\left[ \left(t_1^2-\frac{\gamma^2}{4}\right) \right.\right. \\ &\quad \left.\left. + \left(t_3+t_2\mathrm{e}^{\mathrm{i}k}\right)\left(t_2+t_3\mathrm{e}^{-\mathrm{i}k}\right)\right]\right\}. \end{aligned} \tag{3}$$

When $t_3 = 0$, the winding vector is $t_1^2 - \gamma^2/4 + t_2^2\mathrm{e}^{\mathrm{i}k}$. We obtain the transition points $t_1^2 - \gamma^2/4 = t_2^2$, namely, $t_1 = \pm\sqrt{t_1^2+\gamma^2/4}$ which is just the results obtained in Ref. [10]. When $t_3 \neq 0$, the winding vector is $t_1^2 - \gamma^2/4 - 2t_2t_3 - t_2^2\mathrm{e}^{\mathrm{i}k} - t_3^2\mathrm{e}^{-\mathrm{i}k}$ and the transition points are $t_1 = \pm\left[\gamma^2/4+(t_2+t_3)^2\right]^{1/2}$ and $t_1 = \pm\left[\gamma^2/4-(t_2-t_3)^2\right]^{1/2}$. When the parameters are taken to be $t_2 = 1$, $t_3 = 1/5$, and $\gamma = 4/3$, the transition points should be $t_1 = \pm 1.3728$ which are different from the numerical result $t_1 = \pm 1.56$ given in Ref. [10]. This method becomes inapplicable as soon as $t_3$ becomes nonzero. So it may be applicable to a class of model. Numerical calculation on the generalized Brillouin zone is always effective to find the phase transition points, where a precise formula is been used.

## 4. Coupled SSH model

To verify the effectiveness of the above method, we study the coupled SSH model shown in Fig. 1(b). The model originates from the two-row limit of the brick-wall lattice which is an alternative representation of a honeycomb lattice.[31,32] The coupled SSH system, as the crossover from 1D to 2D system, hosts a rich phase diagram which is different from that of both 1D and 2D systems.[33,34] The non-Hermitian version of the coupled SSH system is studied by introducing the non-Hermitian topological invariants of real space in the

presence of non-Hermitian skin effect.[12] Here, we study the non-Hermitian coupled SSH model without the non-Hermitian skin effect due to the introduction of site dependence hopping terms.

The Bloch Hamiltonian reads $H=\psi_k^\dagger H_k \psi_k$ with

$$H_k = H_{\mathrm{h},k} + H_{\mathrm{nh},k}, \tag{4}$$

where $\psi_k^\dagger = \left(\begin{array}{cccc} a_k^\dagger & b_k^\dagger & c_k^\dagger & d_k^\dagger \end{array}\right)$. The Hermitian part of $H_k$ is given by

$$H_{\mathrm{h},k} = \begin{pmatrix} 0 & \frac{t_1}{2}+t_3\mathrm{e}^{\mathrm{i}k} & 0 & \frac{t_1}{2}+t_2\mathrm{e}^{-\mathrm{i}k} \\ \frac{t_1}{2}+t_3\mathrm{e}^{-\mathrm{i}k} & 0 & \frac{t_1}{2}+t_2\mathrm{e}^{\mathrm{i}k} & 0 \\ 0 & \frac{t_1}{2}+t_2\mathrm{e}^{-\mathrm{i}k} & 0 & \frac{t_1}{2}+t_3\mathrm{e}^{\mathrm{i}k} \\ \frac{t_1}{2}+t_2\mathrm{e}^{\mathrm{i}k} & 0 & \frac{t_1}{2}+t_3\mathrm{e}^{-\mathrm{i}k} & 0 \end{pmatrix},$$

and the non-Hermitian part of $H_k$ is given by

$$H_{\mathrm{nh},k} = \frac{\gamma}{2}\begin{pmatrix} 0 & \mathrm{e}^{\mathrm{i}k} & 0 & 0 \\ -\mathrm{e}^{-\mathrm{i}k} & 0 & 0 & 0 \\ 0 & 0 & 0 & -\mathrm{e}^{-\mathrm{i}k} \\ 0 & 0 & \mathrm{e}^{\mathrm{i}k} & 0 \end{pmatrix}.$$

The coupled SSH Hamiltonian $H_k$ in Eq. (4) also has the chiral symmetry which is the same as that of the SSH Hamiltonian $H_k$ in Eq. (1).

We also calculate the open-boundary spectra with and without non-Hermitian skin effect, as well as the corresponding spectra of $H^\dagger H$ numerically, and find that the above conclusions remain unchanged. Now we find the topological invariant and study the topological transition points. With the unitary matrix

$$U = \begin{pmatrix} 1 & 0 & 0 & 0 \\ 0 & 0 & 1 & 0 \\ 0 & 1 & 0 & 0 \\ 0 & 0 & 0 & 1 \end{pmatrix},$$

the Hamiltonian $H_k$ in Eq. (4) can be tranformed into block off-diagonal form

$$\bar{H}_k = UH_kU^{-1} = \begin{pmatrix} 0 & V \\ V^* & 0 \end{pmatrix},$$

where

$$V = \begin{pmatrix} \frac{1}{2}t_1+\mathrm{e}^{\mathrm{i}k}\left(\frac{1}{2}\gamma+t_3\right) & \frac{1}{2}t_1+t_2\mathrm{e}^{-\mathrm{i}k} \\ \frac{1}{2}t_1+t_2\mathrm{e}^{-\mathrm{i}k} & \frac{1}{2}t_1+\mathrm{e}^{\mathrm{i}k}\left(t_3-\frac{1}{2}\gamma\right) \end{pmatrix}.$$

With the block off-diagonal Hamiltonian $V$, the winding number is given by

$$\mathcal{W} = -\oint \frac{\mathrm{d}k}{2\pi\mathrm{i}}\partial_k\left[\ln\left(\mathrm{Det}V\right)\right],$$

and the winding vector

$$\mathrm{Det}V = t_1t_3\mathrm{e}^{\mathrm{i}k} + \mathrm{e}^{2\mathrm{i}k}\left(t_3^2-\gamma^2/4\right) - t_1t_2\mathrm{e}^{-\mathrm{i}k} - t_2^2\mathrm{e}^{-2\mathrm{i}k}.$$

According to the geometrical meaning of winding vector $\mathrm{Det}V$, the topological phase transistion points are

$$t_1 = \pm\left[(t_2+t_3)+\frac{\gamma^2}{4(t_2-t_3)}\right].$$

When the non-Hermitian skin effect exists in the model, the Bloch-Hamiltonian energy gap closes at $t_1=\pm(t_2+t_3)\pm\gamma/2$ and the system has four topological transition points $t_1=\pm1.15, \pm1.25$ with $t_2=1, t_3=0.2, \gamma=0.1$.[12] However, zero modes open-boundary spectra exist for $t_1\in[-1.21,\ 1.21]$, which is consistent with the critical points estimated by non-Hermitian topological invariants based directly on real-space wavefunctions.[12] Here, we give the topological phase transition points $t_1=\pm1.2031$ when the above parameters are used.

## 5. Conclusions

We have proposed a way to construct the topological invariant of a non-Hermitian system. This method suggests the topological invariants of the original models with non-Hermitian skin effect could be obtained from their partners without non-Hermitian skin effect by adjusting the asymmetric hoppings. When the topological structure of the open-boundary spectra of the modified Hamilton $H_k$ is consistent with that of $H_k^\dagger H_k$, the bulk topological invariants based on the band-theory framework are effective to determine the zero-energy edge states. The winding numbers in analytical form of two non-Hermitian SSH models are obtained to verify the practicality of the method. The merit of the present approach is the simplicity and the possible analytic solutions. The demerit is complexity due to the enlarged Hilbert space. The method presented here can be applied to a rich variety of non-Hermitian systems. However, not all non-Hermitian models can be removed by this simple way. For the models that cannot find the partners, one still has to use the generalized Brillouin zone though numerical calculation, in which a precise formula has been given. There are many open questions ahead. For example, what is the true partner of the non-Hermitian SSH model including the $t_3$ term. How to construct the partner of the non-Hermitian domain-wall model and other non-Hermitian system.

## References


[1] Hasan M Z and Kane C L 2010 *Rev. Mod. Phys.* **82** 3045
[2] Qi X L and Zhang S C 2011 *Rev. Mod. Phys.* **83** 1057
[3] Lee T E 2016 *Phys. Rev. Lett.* **116** 133903
[4] Ye X 2018 *Journal of Physics Communications* **2** 035043
[5] Flore K K, Elisabet E, Jan C B and Emil J B 2018 *Phys. Rev. Lett.* **121** 026808
[6] Martinez A V M ,Barrios V J E,Berdakin M and Foa T L E F 2018 *Eur. Phys. J. Spec. Top.* **227** 1295
[7] Zhou H Y and Lee J Y 2019 *Phys. Rev. B* **99** 235112
[8] Liu C H and Chen S 2019 *Phys. Rev. B* **100** 144106
[9] Liu C H, Jiang H and Chen S 2019 *Phys. Rev. B* **99** 125103

[10] Yao S Y and Wang Z 2018 *Phys. Rev. Lett.* **121** 086803
[11] Kazuki Y and Shuichi M 2019 *Phys. Rev. Lett.* **123** 066404
[12] Song F, Yao S Y and Wang Z 2019 *arXiv* **1905** 02211[cond-mat.mes-hall]
[13] Deng T S and Yi W 2019 *Phys. Rev. B* **100** 035102
[14] Yao S Y, Song F and Wang Z 2018 *Phys. Rev. Lett.* **121** 136802
[15] Xiao L, Deng T S, Wang K K, Zhu G Y, Wang Z, Yi W and Xue P 2019 *arXiv* **1907** 12566[cond-mat.mes-hall]
[16] Tobias H, Tobias H, Stefan I, Mohamed A, Tobias K, Laurens W M, Ching H L, Alexander S, Martin G and Ronny T 2019 *arXiv* **1907** 11562 [cond-mat.mes-hall]
[17] Jin L and Song Z 2019 *Phys. Rev. B* **99** 081103
[18] Ali M 2002 *J. Math. Phys.* **43** 205
[19] Carl M B and Stefan B 1998 *Phys. Rev. Lett.* **80** 5243
[20] Wu H C, Jin L and Song Z 2019 *Phys. Rev. B* **100** 155117
[21] Daniel L, Konstantin Y B, Chunli H, Chong Y D and Franco N 2017 *Phys. Rev. Lett.* **118** 040401
[22] Yin C H, Jiang H, Li L H, Lü R and Chen S 2014 *Phys. Rev. A* **97** 052115
[23] Han Y Z, Jiang H, Chen S and Liu C S 2019 *Physica E* **110** 68-73
[24] Simon L 2018 *Phys. Rev. B* **97** 045106
[25] Shen H, Zhen B and Fu L 2018 *Phys. Rev. Lett.* **120** 146402
[26] Li C, Zhang X Z, Zhang G and Song Z 2018 *Phys. Rev. B* **97** 115436
[27] Rudner M S and Levitov L S 2009 *Phys. Rev. Lett.* **102** 065703
[28] Jiang H, Yang C and Chen S 2018 *Phys. Rev. A* **98** 052116
[29] Gurarie V 2011 *Phys. Rev. B* **83** 085426
[30] Wang Z and Zhang S C 2014 *Phys. Rev. X* **4** 011006
[31] Alexei K 2006 *Ann. Phys.* **321** 2
[32] Feng X Y, Zhang G M and Xiang T 2007 *Phys. Rev. Lett.* **98** 087204
[33] Yasuhiro S, Satoshi A, Takaaki J, Masayuki I and Yutaka U 2015 *Phys. Rev. Lett.* **114** 166403
[34] Sangmo C, Kim T, Lee S and Han W Y 2015 *Phys. Rev. Lett.* **350** 182